

Crystal Structure of $\text{Fe}_2\text{P}_2\text{O}_7$

J. T. HOGGINS*

*Ventures Research Division, Ashland Chemical Company,
Dublin, Ohio 43017*

J. S. SWINNEA AND H. STEINFINK

*Material Science and Engineering Laboratories, Department of Chemical
Engineering, The University of Texas at Austin, Austin, Texas 78712*

Received October 21, 1982; in revised form December 27, 1982

$\text{Fe}_2\text{P}_2\text{O}_7$ crystallizes in the $C\bar{1}$ space group with lattice parameters $a = 6.649(2) \text{ \AA}$, $b = 8.484(2) \text{ \AA}$, $c = 4.488(1) \text{ \AA}$, $\alpha = 90.04^\circ$, $\beta = 103.89(3)^\circ$, $\gamma = 92.82(3)^\circ$, and $\rho_{\text{cal}} = 3.86 \text{ g/cc}$. It is essentially isostructural with $\beta\text{-Zn}_2\text{P}_2\text{O}_7$. As in the Zn compound, the bridging oxygen atom in the P_2O_7 group shows a high anisotropic thermal motion. It appears that the P-O-P bond angle is linear as a result of extensive π bonding with the p orbitals on the bridging oxygen atom. The high thermal motion is vibration of the atom into cavities in the structure.

Introduction

This paper reports the crystal structure of $\text{Fe}_2\text{P}_2\text{O}_7$. This compound is one in a series of related pyrophosphates having the thortveitite structure (1) for their high temperature form. This series includes $\text{Mn}_2\text{P}_2\text{O}_7$ (2), $\text{Cu}_2\text{P}_2\text{O}_7$ (3), $\text{Mg}_2\text{P}_2\text{O}_7$ (4), and $\text{Zn}_2\text{P}_2\text{O}_7$ (5). A phase transformation is reported for all of these compounds except Mn. $\text{Fe}_2\text{P}_2\text{O}_7$ is isostructural with the high temperature forms of the above phases. The melting point of this compound is approximately 1200°C .

Experimental

The $\text{Fe}_2\text{P}_2\text{O}_7$ material for this analysis was prepared by mixing aqueous solutions

of $\text{FeNO}_3 \cdot 9\text{H}_2\text{O}$ and $(\text{NH}_4)_2\text{HPO}_4$. The solution was evaporated to dryness and the residue was subsequently heated to 250°C to decompose NH_4NO_3 . The material was then heated at 500°C for 2 days. The result of this reaction was FePO_4 as shown by the X-ray powder diffractogram. The FePO_4 was reduced in a vycor tube by heating it at 450°C for 2 days in an atmosphere of wet H_2 . Crystals of $\text{Fe}_2\text{P}_2\text{O}_7$ were grown by sealing the above material in evacuated silica tubes, heating to 1265°C for 1 day, and slowly cooling at a rate of $83^\circ\text{C}/\text{day}$ to 850°C . The Mössbauer spectrum of this material showed a single quadrupole split line with an isomer shift of 1.22 mm/sec with respect to iron and a quadrupole splitting of 2.44 mm/sec .

An irregularly shaped, colorless crystal approximately $0.050 \times 0.075 \times 0.100 \text{ mm}$ was selected for structure analysis. It was mounted on a Syntex single crystal autodif-

* Author to whom correspondence is to be addressed.

fractometer, and $\text{MoK}\alpha$ radiation monochromatized with a graphite crystal was used in the data collection. From an initial rotation photograph around an arbitrary axis, 2θ and χ positions for 15 reflections were obtained. These reflections were then located by searching ϕ and were centered at their Bragg positions. An autoindexing routine was used to obtain possible unit cells. An examination of the solutions suggested a unit cell with dimensions similar to those of $\beta\text{-Mg}_2\text{P}_2\text{O}_7$ (4). However, examination of reciprocal space symmetry and the least squares refinement of the cell parameters indicated that the proper crystal system for $\text{Fe}_2\text{P}_2\text{O}_7$ was triclinic and not monoclinic as for $\beta\text{-Mg}_2\text{P}_2\text{O}_7$.

Refined lattice constants based on 46 reflections whose 2θ values were precisely determined in the range $15^\circ \leq 2\theta \leq 30^\circ$ are $a = 6.649(2) \text{ \AA}$, $b = 8.484(2) \text{ \AA}$, $c = 4.488(1) \text{ \AA}$, $\alpha = 90.04(3)^\circ$, $\beta = 103.89(3)^\circ$, and $\gamma = 92.82(3)^\circ$. The monoclinic cell parameters for $\beta\text{-Mg}_2\text{P}_2\text{O}_7$ at 95°C are $a = 6.494(7) \text{ \AA}$, $b = 8.28(1) \text{ \AA}$, $c = 4.522(5) \text{ \AA}$, and $\beta = 103.8(1)^\circ$ (4). The monoclinic cell parameters reported by Calvo (5) for $\beta\text{-Zn}_2\text{P}_2\text{O}_7$ are also closely related to those of $\text{Fe}_2\text{P}_2\text{O}_7$. Intensity data were collected to $2\theta = 55^\circ$ by the variable ω -scan technique at rates from 2.0 to 5.0 min^{-1} ; more time was devoted to less intense reflections. The measured intensities were corrected for Lorentz and polarization effects as well as absorption using $\mu_l = 66.78 \text{ cm}^{-1}$. The transmission factors ranged from 0.52 to 0.68 . Estimated errors of the intensities were calculated from $\sigma(F^2) = [S^2(I_p + 1/R^2(I_{B_1} + I_{B_2})) + (pI_{hkl})^2]^{1/2}$, where I_p is the number of counts accumulated during the scan of the peak, I_{B_1} = background counts on low 2θ side, I_{B_2} = background counts on high 2θ side, S = scan speed in deg/min , R = ratio of total background counting time to scan time, $p = 0.02$ (6), and $I_{hkl} = S[I_p - 1/R(I_{B_1} + I_{B_2})]$. Of the 561 intensities collected, 505 were considered observed on the basis that F ex-

ceeded $2\sigma(F)$. Intensity statistics were in excellent agreement with a centrosymmetric distribution and $\text{C}\bar{1}$ was chosen as the space group. The C centered cell was retained for ease of comparison to previously determined structures.

Structure Determination

A three-dimensional Patterson map calculated from the 505 observed intensities was found to be consistent with Fe and P atoms in the Mg and P positions of $\beta\text{-Mg}_2\text{P}_2\text{O}_7$. An electron density map based on phases generated from these two positions immediately led to the location of the four oxygen positions. Full matrix least squares refinement using the program NUCLS (7) and isotropic temperature factors converged to $R = 0.092$ ($\omega R = 0.104$). The function minimized in the refinement was $\Sigma\omega(F_o - F_c)^2$, where the weights ω are $[\sigma(F_o)]^{-2}$. Values of the scattering factors for neutral atoms corrected for the real and imaginary parts of dispersion were used (8). Least squares refinement incorporating anisotropic temperature factors and an isotropic extinction correction ($g = 1.6 \times 10^{-5}$) converged to $R = 0.039$ ($\omega R = 0.045$) for the 505 observed reflections and $R = 0.045$ ($\omega R = 0.046$) for all 561 reflections. A final electron density map showed random peaks and depressions, the largest amplitude being about $\pm 1 e \text{ \AA}^3$. The final atomic parameters are shown in Table I, and Table II contains the observed and calculated structure amplitudes.¹

¹ See NAPS document No. 04060 for 3 pages of supplementary material. Order from ASIS/NAPS, Microfiche Publications, P.O. Box 3513, Grand Central Station, New York, NY 10163. Remit in advance \$4.00 for microfiche copy or for photocopy, \$7.75 up to 20 pages plus \$.30 for each additional page. All orders must be prepaid. Institutions and organizations may order by purchase order. However, there is a billing and handling charge for this service of \$15. Foreign orders add \$4.50 for postage and handling, for the first 20 pages, and \$1.00 for additional 10 pages of material. Remit \$1.50 for postage of any microfiche orders.

TABLE I
 $\text{Fe}_2\text{P}_2\text{O}_7$ POSITIONAL PARAMETERS AND THERMAL VIBRATIONS ($\times 10^4$) (STANDARD DEVIATIONS ARE IN PARENTHESES)^a

Atom	<i>x</i>	<i>y</i>	<i>z</i>	β_{11}	β_{22}	β_{33}	β_{12}	β_{13}	β_{23}
Fe	96(1)	3101(1)	4830(2)	79(2)	24(1)	128(5)	-5(1)	-31(2)	4(1)
P	7884(2)	-6(2)	899(3)	23(3)	47(2)	80(7)	0(2)	0(4)	12(3)
O1	0	0	0	21(16)	561(36)	320(47)	40(20)	77(23)	134(33)
O2	3748(6)	47(4)	2148(8)	34(9)	40(5)	69(18)	9(5)	-13(10)	7(8)
O3	7892(8)	1487(5)	2741(10)	187(14)	30(6)	181(22)	-23(7)	-44(14)	9(8)
O4	2745(6)	3527(5)	2782(9)	105(11)	33(5)	143(21)	33(6)	6(12)	9(8)

^a The temperature factor is $\exp[-(\beta_{11}h^2 + \beta_{22}k^2 + \beta_{33}l^2 + 2(\beta_{12}hk + \beta_{13}hl + \beta_{23}kl))]$.

Discussion

The $\text{Fe}_2\text{P}_2\text{O}_7$ parameters, when compared with the parameters for $\beta\text{-Mg}_2\text{P}_2\text{O}_7$ reported by Calvo, indicate that both structures are very similar. The oxygen atoms labeled O3 and O4 in Table I correspond to Calvo's O3 in space group $C2/m$. It is interesting that Calvo remarks on the nonpositive definite values of his thermal matrices and thought it "suggestive of erroneous space group choice." He attempted refinement in $C2$ but was unsuccessful. It may well be that the correct space group for $\beta\text{-Mg}_2\text{P}_2\text{O}_7$ is $C1$.

The bond distances and angles are listed in Tables III and IV, respectively. Since $\text{Fe}_2\text{P}_2\text{O}_7$ is essentially isostructural with $\text{Sc}_2\text{Si}_2\text{O}_7$ and $\text{Zn}_2\text{P}_2\text{O}_7$, only the highlights will be given here. This structure can be described as distorted close-packed layers of oxygen atoms parallel to the *ab* plane. The cations (Fe) fill $\frac{2}{3}$ of the octahedral voids. Thus each Fe-O octahedron shares three edges to form a network. Each oxygen in the sheets is bonded to two iron atoms and one phosphorus. The pyrophosphate groups bridge these sheets and lie opposite the vacant octahedral void. The base of each P-O tetrahedron is formed from two oxygen atoms from one oxygen net and one oxygen from the next net. The bridging oxygen in the pyrophosphate lies

between the close packed layers and bonds only to the two phosphorus atoms.

The structure is relatively open along the *b* direction near the bridging oxygens. From the center of these holes to the nearest neighbor is approximately 4 Å. These holes link to form channels through the structure. In Fig. 1 is shown a stereoscopic view of the structure which emphasizes the channels.

The enhanced thermal vibration of O1 perpendicular to the P-P line and approximately parallel to the *b* axis was also noted for this atom in $\text{Mg}_2\text{P}_2\text{O}_7$ and $\text{Zn}_2\text{P}_2\text{O}_7$ (4, 5). Based on the sum of the bond strengths, as developed by Brown and Shannon (9), and geometric considerations it is possible to get some insight as to whether this temperature factor is due to a static or dynamic disorder. If static, and if each P-O bond for bridging oxygen has a bond strength of 1.0 valence unit (vu), then this bond length is 1.635 Å. To maintain $\Sigma S(\text{P}) = 5.0$, the P atom must move closer to the other three oxygen atoms. These bonds need to become approximately 0.02 Å shorter, requiring the phosphorus atom to move about 0.05 Å along the P-P direction. Given the above conditions, the bridging oxygen would be approximately 0.27 Å from the P-P line and the P-O-P angle would be about 160°. These shifts and resulting bond length differences are well outside the standard

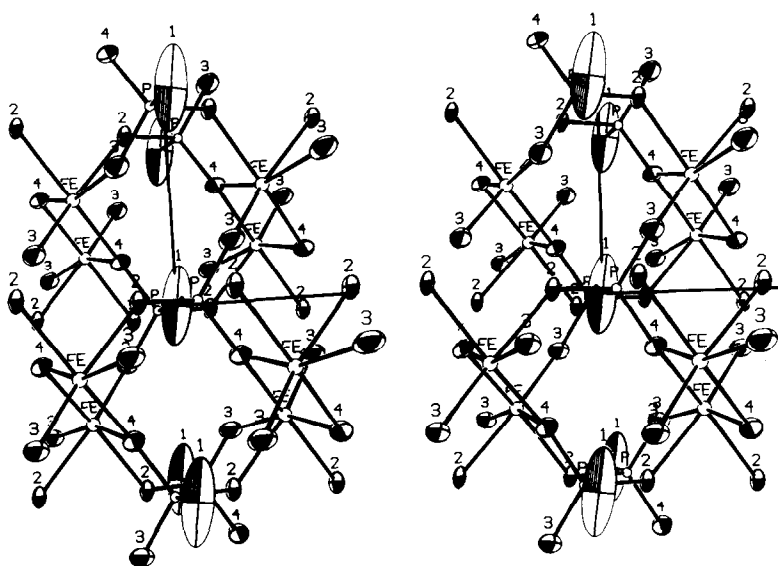


FIG. 1. Stereoscopic view of the $\text{Fe}_2\text{P}_2\text{O}_7$ structure. The c axis is horizontal, $\frac{1}{2}b$ is drawn vertical and $-\frac{1}{2}a$ extends towards the viewer.

deviations for this structure. If the large thermal vibration is due to a static disorder, $\Sigma S(\text{P})$ should then be significantly greater than 5.0. As indicated above, there are large cavities in the structure adjacent to the bridging oxygens in the direction of the large component of thermal vibration and it may well be that the temperature factor is a true dynamic effect.

The high valency on the bridging oxygen may be due to extensive $p-\pi$ bonding. Brown and Shannon (9) noted that the bond strength sums around bridging oxygen atoms in pyrophosphate groups increase as the $\text{P}-\text{O}-\text{P}$ angle increases. Cruickshank (10) discussed the role of 3-d orbitals in π bonding in phosphates. He noted that the opening of the $\text{P}-\text{O}-\text{P}$ angle allows a second π system to become increasingly important, and at 180° the bridging oxygen will have two p orbitals that may join fully in the π systems. The net result is that the strength of this bond increases with the additional π bonding. Thus, for a $\text{P}-\text{O}-\text{P}$ angle of 180° there is extensive $p-\pi$ interaction with a corresponding bond strength

approximately 1.2 valence units and a $\text{P}-\text{O}$ bond distance of $\sim 1.55 \text{ \AA}$. For a $\text{P}-\text{O}-\text{P}$ angle of $\sim 124^\circ$ there is little $p-\pi$ bonding with a corresponding bond strength of 1.0 vu and a bond distance of $\sim 1.61 \text{ \AA}$.

The Fe octahedron irregularity and the long $\text{Fe}-\text{O}_3$ bond correspond to similar observations for the $\text{Mg}-\text{O}$ octahedron in the $\beta\text{-Mg}_2\text{P}_2\text{O}_7$ structure (4). Calvo's discussion concerning the reasons for the octahedral distortion appears to be also applicable to $\text{Fe}_2\text{P}_2\text{O}_7$.

Addendum

One of the reviewers pointed out to us that a paper by T. Stefanidis and A. G. Nord appeared in *Z. f. Kristallogr.* **159**, 255 (1982) dealing with the crystal structure of $\text{Fe}_2\text{P}_2\text{O}_7$. They refined the structure in $\text{P}1$ and report $R = 0.049$.² Their choice of space group is based on the statistical dis-

² The transformation between the C and P cells is 110/-110/001.

TABLE III
DISTANCES AND FORCES BETWEEN ATOMS IN
Fe₂P₂O₇

Bond	<i>d</i> (Å)	Bond strength <i>s</i> (vu) ^{a,b}	Valence <i>v</i> (vu) ^{a,b}
Fe–O2' ^c	2.068(4) ^d	0.40	
–O2'	2.147(4)	0.33	
–O3'	2.523(5)	0.14	
–O3	2.012(5)	0.46	
–O4'	2.139(4)	0.34	
–O4	2.190(4)	0.30	1.97
P–O1	1.554(1)	1.18	
–O2'	1.528(4)	1.24	
–O3	1.511(4)	1.29	
–O4'	1.517(4)	1.27	4.98
O1–2P	1.554	1.18	2.36
O2–P	1.528	1.24	
–Fe	2.068	0.40	
–Fe	2.147	0.33	1.97
O3–P	1.511	1.29	
–Fe	2.523	0.14	
–Fe	2.012	0.46	1.89
O4–P	1.517	1.27	
–Fe	2.139	.34	
–Fe	2.190	.30	1.91

^a vu = valence unit.

^b $V = \Sigma S = \Sigma S_0(R/R_0)^{-N}$; for Fe: $S_0 = 0.5$; $R_0 = 1.981$; $N = 5.2$; for P: $S_0 = 1.25$; $R_0 = 1.525$; $N = 3.2$.

^c Atoms indicated with primes are symmetry related to those shown in Table I.

^d Standard deviations are in the parentheses.

tributions of the structure factors. The statistics for our data agree very closely with a centrosymmetric distribution. Further, their Table II clearly shows an x and \bar{x} relationship for Fe(1) and Fe(2), P(1) and P(2), and for oxygen atoms such as O(1)–O(7) and O(2)–O(6). In the least squares refinement the correlation coefficients between these parameters must have been very large, although the authors make no mention of it. In the discussion of the structure the authors also indicate their discomfort with the distortions of the O–P–O angles. They express the suspicion that “the bridging oxygen O(4) . . . has been slightly

misplaced . . . even if the refined atomic parameters for O(4) do not give a very strong support to this idea.” Even though P–O(4)–P is no longer linear in their structure, the thermal vibration of this oxygen remains very large. We had refined our structure to $R = 0.033$, $\omega R = 0.038$ using the acentric space group. However, 217 terms of 4560 independent elements of the correlation matrix have values greater than ± 0.5 and those between positional parameters are near 1. Furthermore, the thermal parameters of 7 of the 11 “independent” atoms were not positive definite. The centrosymmetric refinement converges to $\omega R = 0.045$ and although Hamilton’s ratio test indicates that the noncentrosymmetric refinement is significant at the 95% confidence level, we reject it on the basis of the statistics of the structure factors, the large number of highly correlated parameters and the nonpositive-definite thermal parameters. The question as to the true configuration of P–O–P in P₂O₇ is certainly not settled, but on the basis of the data which we used in our analysis the bridging oxygen must be placed in line with the P atoms.

TABLE IV
BOND ANGLES FOR Fe₂P₂O₇ (STANDARD DEVIATIONS
IN PARENTHESES)

Angles (°)			
O2'–Fe–O2''	79.71(14)	O2'''–P–O1'	105.04(16)
O3'–Fe–O2''	95.12(16)	O3–P–O1'	107.00(22)
O3''–Fe–O2''	80.62(14)	O3–P–O2'''	112.82(24)
O3'–Fe–O2'	78.00(15)	O4'–P–O1	106.91(18)
O3''–Fe–O3	75.85(17)	O4'–P–O2'''	112.58(22)
O4'–Fe–O2'	94.38(15)	O4'–P–O3	111.91(24)
O4–Fe–O2'	88.46(15)		
O4–Fe–O2''	86.24(15)		
O4–Fe–O3	116.98(18)		
O4'–Fe–O3''	113.95(15)		
O4'–Fe–O3	96.93(17)		
O4'–Fe–O4	77.65(15)		

Acknowledgments

The authors thank Denise A. Dale and Corbett Taylor for their assistance in preparing this material and Fred Ruzala for his helpful discussions.

References

1. D. W. J. CRUICKSHANK, H. LYNTON, AND G. A. BARCLAY, *Acta Crystallogr.* **15**, 491 (1962).
2. K. LUKASZEWICZ AND R. SMAJKIEWICZ, *Rocz. Chem.* **35**, 741 (1961).
3. B. E. ROBERTSON AND C. CALVO, *Acta Crystallogr.* **22**, 665 (1967).
4. C. CALVO, *Canad. J. Chem.* **43**, 1139 (1965).
5. C. CALVO, *Canad. J. Chem.* **43**, 1147 (1965).
6. W. R. BUSING AND H. A. LEVY, *J. Chem. Phys.* **26**, 563 (1957).
7. "NUCLS-UT Modified Doeden-Ibers Program."
8. "International Tables for X-ray Crystallography," Vol. IV, Kynoch Press, Birmingham England (1974).
9. I. D. BROWN AND R. D. SHANNON, *Acta Crystallogr.* **A29**, 266 (1973).
10. D. W. J. CRUICKSHANK, *J. Chem. Soc.* **5486**, (1961).